

UNCLASSIFIED

**Defense Technical Information Center
Compilation Part Notice**

ADP011190

TITLE: High Birefringence Liquid Crystals for Laser Beam Steering

DISTRIBUTION: Approved for public release, distribution unlimited

This paper is part of the following report:

TITLE: The Annual AIAA/BMDO Technology Conference [10th] Held in Williamsburg, Virginia on July 23-26, 2001. Volume 1. Unclassified Proceedings

To order the complete compilation report, use: ADB273195

The component part is provided here to allow users access to individually authored sections of proceedings, annals, symposia, etc. However, the component should be considered within the context of the overall compilation report and not as a stand-alone technical report.

The following component part numbers comprise the compilation report:

ADP011183 thru ADP011193

ADP204784 thru ADP204818

UNCLASSIFIED

HIGH BIREFRINGENCE LIQUID CRYSTALS FOR LASER BEAM STEERING

Shin-Tson Wu

HRL Laboratories, LLC, 3011 Malibu Canyon Road, Malibu, CA 90265

Abstract

High birefringence and low viscosity liquid crystals are crucial for improving the response time of an agile laser beam steering device. Nematic liquid crystals with birefringence greater than 0.4, low absorption and good photo and thermal stability are investigated.

Introduction

The optical phased arrays (OPA) developed by Raytheon and AFRL, as shown in Fig.1, is a versatile device for laser beam steering and optical communications.¹ The applied stepwise voltages create liquid crystal (LC) phase grating that deflects the incoming laser beam to a programmable angle with high precision. To steer a $\lambda=1.55\mu\text{m}$ laser beam, the required 2π phase change ($\delta=2\pi d\Delta n/\lambda$) leads to $d\Delta n\sim 1.6$; d is the LC layer thickness. Although a thick LC layer would lead to a large phase shift, its response time is sluggish because the LC response time is proportional to d^2 . In order to achieve fast response time while keeping high manufacturing yield, the cell gap is normally kept at $d\sim 4\mu\text{m}$. Thus, LC mixtures with $\Delta n\geq 0.4$ and low viscosity, low optical loss, wide nematic range, and low operating voltage are desperately needed.

To compare the performance among various LC compounds, we have defined a figure-of-merit (FoM) as following:²

$$FoM = K_{11}(\Delta n)^2 / \gamma_1 \quad (1)$$

In Eq.(1), K_{11} is the splay elastic constant and γ_1 is the rotational viscosity. Since K_{11} , Δn and γ_1 are all dependent on the temperature, FoM is sensitive to the operating temperature. In the low temperature regime,

as the temperature is increased, the decreasing rate of γ_1/K_{11} is much faster than that of $(\Delta n)^2$ resulting in an enhanced FoM. As the temperature gets close to the clearing point (T_c) of the LC employed, the decreasing rate of γ_1/K_{11} gradually saturates while $(\Delta n)^2$ starts to decrease rapidly. As a result, FoM drops sharply as the temperature approaches T_c . Therefore, FoM has a maximum value at a temperature called optimal operating temperature (T_{op}). For a given LC mixture, T_{op} is about 20°C below T_c . Operating an OPA at a higher temperature would boost FoM, however, the long-term stability of the driving electronics and LC medium should be taken into consideration.

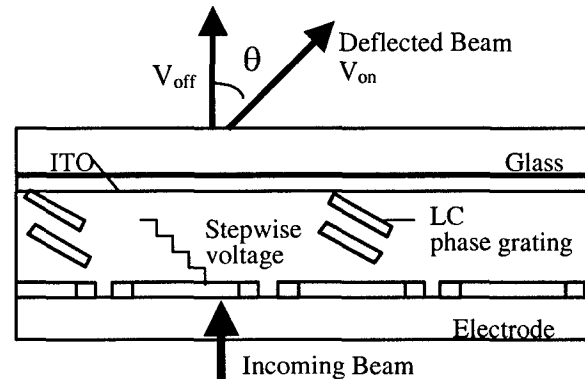


Fig.1 A sketch of a LC-based optical phased array. The applied stepwise voltage generates LC phase grating that deflects the incoming laser beam.

For laser beam steering, our objective is to develop new liquid crystal mixtures exhibiting $FoM > 70$ $\text{ms}/\mu\text{m}^2$ at $T < 70^\circ\text{C}$ while possessing good photo and thermal stability, low operating voltage and low absorption loss.

The information contained in this material is unclassified, technically accurate, nonproprietary and considered suitable for public release. It contains no computer software, owned or developed by or for the government. Export restrictions (i.e., MCTL, Munitions List (ITAR and CCL) and current AF/DoD policy have been considered prior to requesting public release approval.

LC Birefringence

Based on the single band model, the LC birefringence is expressed as:³

$$\Delta n = G \frac{\lambda^2 \lambda^{*2}}{\lambda^2 - \lambda^{*2}} \quad (2)$$

In Eq.(1), $G \sim NZS(f_{\parallel} - f_{\perp})$, where N is the molecular packing density, Z is the number of participating electrons, S is the order parameter that governs the temperature effect, $(f_{\parallel} - f_{\perp})$ is the differential oscillator strength, and λ^* is the mean resonance wavelength. From Eq.(2), the LC birefringence is mainly determined by the molecular conjugation length, differential oscillator strength (i.e., molecular shape and size), and temperature. When the temperature is far below the clearing point, the order parameter can be approximated by:⁴

$$S = (1 - T/T_c)^{\beta} \quad (3)$$

For many LC compounds studied, $\beta \sim 0.25$ is nearly a constant and is insensitive to materials.

Based on Eqs. (2) and (3), an effective way for increasing Δn is to search for short chain and linearly conjugated molecules. Such linear LC compounds tend to exhibit high Δn , relatively low viscosity and high clearing point. A major drawback of the highly conjugated compounds is high melting point. A well known example is 5CT (cyano-terphenyl); its nematic range is from 131°C to 240°C. Therefore, in order to lower the melting point to -40°C for storage purpose, eutectic mixtures consisting of more than 10 components are rather common.

Another serious concern for high birefringence LCs is their photo and thermal stability. To prevent LC material from interacting with moistures, a LC cell is hermetically sealed. An incoherent UV light is used to cure the glue lines before injecting LC mixture and then plug the hole after vacuum filling the LC device. Thus, the LC material has to withstand at least 30 seconds of intense UV exposure (I~100mw/cm²) without degradation. Moreover, the LC device is expected to operate at elevated temperatures in order to obtain high speed, excellent thermal stability is another important criterion.

In the visible spectral region, Δn decreases as the wavelength increases. For an OPA operating at $\lambda = 1.55\mu\text{m}$, the condition $\lambda \gg \lambda^*$ holds and Eq.(2) is reduced to $G\lambda^{*2}$, which is insensitive to the

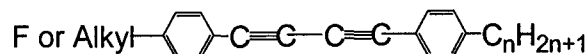
wavelength. That means, the LC birefringence in the near IR region is basically a constant, mainly governed by G and λ^* . For a LC with $\lambda^* = 250\text{nm}$, its Δn at $\lambda = 1.55\mu\text{m}$ is about 23% lower than that at $\lambda = 550\text{nm}$. Therefore, in order to obtain $\Delta n = 0.4$ at $\lambda = 1.55\mu\text{m}$, the compounds should possess $\Delta n \sim 0.5$ at $\lambda = 550\text{nm}$.

LC Compounds with $0.4 < \Delta n < 0.5$

In this category, diphenyl-diacetylenes and tolans are chosen as examples. Diphenyl-diacetylenes exhibit many nice physical properties, however, their photo and thermal stability is inadequate. On the other hand, tolans have better stability except their molecular conjugation is not long enough. An electron acceptor polar group, e.g., CN or NCS needs to be attached for enhancing birefringence.

Diphenyl-diacetylenes (PTTP)

The asymmetric diphenyl-diacetylenic liquid crystals⁵ (abbreviated as PTTP; P=phenyl ring, T= carbon-carbon triple bond), as shown below, exhibit a high Δn , low viscosity and wide nematic range.



Both alkyl, alkenyl, and fluoro PTTP homologues have been synthesized. Replacing the alkyl by an alkenyl side chain dramatically enhances the clearing point and widens the nematic range.⁶ High clearing point also plays an important role in improving birefringence due to higher order parameter. Mixtures consisting of these olefin PTTP homologues exhibit $\Delta n \sim 0.43$ at $\lambda = 633\text{nm}$ and $T = 20^\circ\text{C}$.

Three mixtures (designated as A, B and C) consisting of different PTTP components were formulated and their FoM evaluated at elevated temperatures. Results are compared to a commercial mixture E7 as shown in Fig.2. Mixture A is a eutectic mixture consisting of PTTP-24, -36, -4F and -6F. Its clearing point is 90°C and maximum FoM reaches 20 $\mu\text{m}^2/\text{s}$ at $T \sim 65^\circ\text{C}$. Mixture B is a binary olefin PTTP mixture consisting of 47% PTTP-4d2,F and 53% PTTP-5d2,F. Its clearing point is as high as 163°C and FoM reaches 80 $\mu\text{m}^2/\text{s}$ at $T \sim 80^\circ\text{C}$. Unfortunately, mixture B's melting point is too high (78°C) for practical applications. To lower the melting point, we added some non-polar alkenyl PTTP homologues (PTTP-2,4d2, -2,5d2 and -3,6d2) to form mixture C. The nematic range of mixture C is from 6 to 156°C. Its FoM reaches 40 $\mu\text{m}^2/\text{s}$ at $T \sim 80^\circ\text{C}$.

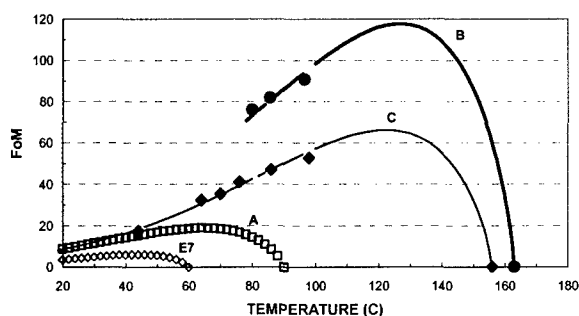


Fig.2 The temperature-dependent FoM (in unit of $\mu\text{m}^2/\text{s}$) of E7, mixtures A, B and C. $\lambda=633\text{ nm}$.

Inadequate photo and thermal stability is a major concern for the PTTP compounds.⁷ Figure 3 shows the measured voltage-dependent transmittance of a homogeneous cell before and after UV exposure. The LC used is PTTP-24/36 binary mixture (50% PTTP-24 and 50% PTTP-36). The UV light intensity was measured to be $I=50\text{mw}/\text{cm}^2$ and central wavelength at $\lambda\sim 365\text{nm}$. Dots represent experimental results at $t=0$ and squares are exposed with UV light for 65 seconds.

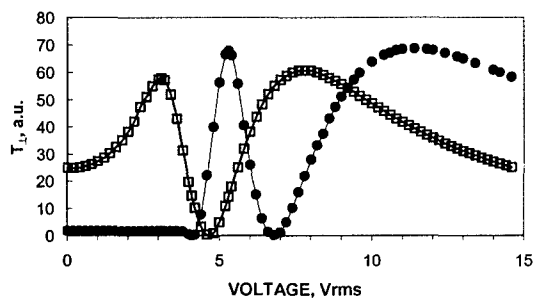


Fig.3 The voltage-dependent transmittance of a homogeneous LC cell before (dots) and after (squares) UV exposure. UV intensity $I=50\text{mw}/\text{cm}^2$. Cell gap $d=3.74\mu\text{m}$, probing laser $\lambda=633\text{nm}$ and $T=22^\circ\text{C}$. Alignment layer is buffed polyimide film. Crossed polarizers. Exposure time=65 seconds.

From Fig.3, three general phenomena are observed when degradation occurs: 1. The effective Δn is decreased, 2. The threshold voltage is smeared and decreased, and 3. The light scattering intensity is increased. The degradation mechanism is believed to originate from the UV-induced free radicals of the diacetylene group. These free radicals transfer charges to the neighboring PTTP molecules, converting triple bond into double bond and initiating the polymerization process from front surface layers and gradually migrating into bulk as UV dosage increases. Once the surface layers are cross-linked, the surface alignment is disturbed resulting in a

reduced Δn , increased viscosity, smeared threshold voltage, and increased light scattering.

Figures 4 (a) and (b) show the photos of a $6\text{-}\mu\text{m}$ homogeneous-aligned LC cell taken under a polarizing optical microscope before and after UV exposure, respectively. Before UV exposure, the cell shows uniform green color between crossed-polarizers. After 85 seconds of exposure at $I\sim 50\text{mw}/\text{cm}^2$, the cell turned to different color and some cross-linking textures appeared. These polymerized clusters scatter light, disturb LC alignment and increase pretilt angle. As a result, the observed birefringence is decreased, and threshold voltage is smeared and reduced.

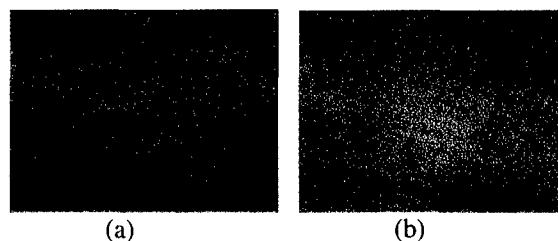
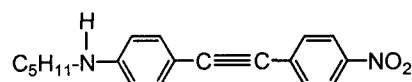


Fig.4 Microscope photos of a $6\text{-}\mu\text{m}$ homogeneous LC cell before (a) and after (b) UV exposure for 85 seconds. Note the color change and polymerized textures in (b).

To retard the polymerization process, an UV scavenger as shown below has been discovered.⁸ Adding 10% of a nitro-amino toluene to PTTP-24/36, the mixture's UV stability is significantly improved.



PTTP Compounds

Since diacetylene causes material instability, these two acetylene groups should be separated. One possibility is to move an acetylene group outside the phenyl rings, as shown below:

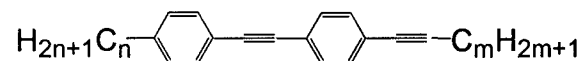


Table I lists the phase transition temperatures of some PTTP compounds.

From Table I, these PTTP compounds exhibit either monotropic phase or no LC phase at all. The monotropic phase is undesirable for mixture applications owing to its high melting temperature. For a normal LC, we prefer low melting and high clearing points.

Table I Phase transition temperatures of some Chisso and Merck PTPT-nm compounds.

n	m	Phase Transition (°C)
2	2	K 83.1 I
2	3	K 89.8 I
3	1	K 87.7 N (85.1) I
3	2	K 100.1 N (48.7) I
3	3	K 78.0 N (54.0) I
3	5	K 72.0 N (40.4) I
4	1	K 81.0 N (56.9) I
4	2	K 87.6 N (76.8) I
4	3	K 100.9 N (65.0) I
4	4	K 84.3 I
5	2	K 80.8 N (46.1) I
5	3	K 76.2 N (50.3) I

The UV absorption spectrum of PTPT-35 (circles) was measured and results are compared with PTTP-24 (squares) as shown in Fig.5. Although these two LCs consist of similar core structure, PTTP seems to have a longer conjugation than the alternating PTPT.

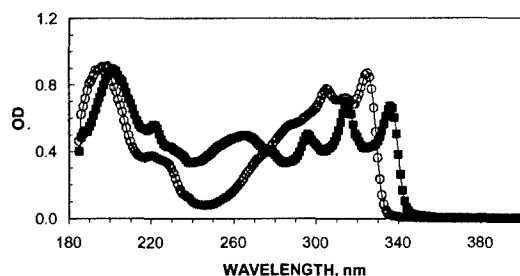


Fig.5. Measured optical density of PTPT-35 (gray) and PTTP-24 (black). Concentration=1%, d=6μm, and host ZLI-2359.

Tolanes (PTP)

Many tolanes derivatives, as shown in Table II, have been studied.⁹ Some cyano (CN) and isothiocyanato (NCS) tolanes exhibit either monotropic or smectic phase so that they are unfavorable for forming nematic mixtures. Replacing the alkyl side chain with an alkenyl group the monotropic phase is converted to enantiotropic nematic phase.¹⁰ Such compounds possess a wide nematic range, lower melting point, and higher Δn as compared to their parent compound. The extrapolated Δn of these tolanes exceeds 0.4.

Both CN and NCS polar groups are effective electron acceptors. They effectively extend the electron conjugation so that the LC birefringence is significantly enhanced. They also possess a large dipole moment (4 Debye for CN and ~3.6 Debye for NCS). However, the cyano compounds tend to form

dimers so that their viscosity is high. Thus, NCS is more favorable than CN for achieving high birefringence, low viscosity, and large dielectric anisotropy. The major challenges of the NCS compounds are in two aspects: 1. Their synthesis procedures are more complicated, and 2. The NCS compounds usually favor smectic phase.

Table II Physical properties of some tolane derivatives. Here, K, N, and I represent crystalline, nematic and isotropic phase, respectively, () stands for monotropic phase transition, Ph in column Y stands for a phenyl ring.

$\text{H}_{2n+1}\text{C}_n\text{-Y-}\langle\text{C}_6\text{H}_4\rangle\text{-C}\equiv\text{C-}\langle\text{C}_6\text{H}_3\text{X}_2\text{X}_3\rangle$						
X ₁	X ₂	X ₃	n	Y	Phase Transitions	Δn
CN	H	H	3	-	K 87 N (78) I	
CN	H	H	3	O	K 98 N 103 I	
CN	H	H	3	≡	K 119 N (87) I	0.46
CN	H	H	3	=	K 100 N 150 I	0.47
CN	F	H	3	≡	K 109 I	0.41
CN	F	H	3	=	K 74 N 102 I	0.43
CN	H	H	4	S	K 80 N (53) I	0.34
NCS	H	H	4	S	K 84.8 SmB 85.4 N (65) I	0.49
NCS	H	H	5	-	K 92 SmA (82) I	
NCS	F	F	4	O	K 71 N (62) I	0.41
NCS	F	F	4	Ph	K 63 SmA 100 N 209 I	0.46

It should be mentioned that the LC compounds containing CN or NCS group usually exhibit a low resistivity. However, recent studies¹¹ show that if at least X₂ or X₃ is a fluoro group, the voltage holding ratio is boosted to 98%. Such fluoro group also contributes to enhance the dielectric anisotropy. The tradeoff is in the increased viscosity.

Figure 3 shows the UV stability of the pentyl-isothiocyanato-tolane (PTP-5NCS). Since PTP-5NCS is smectic, we mixed 20% in an UV transparent nematic mixture ZLI-2359. A 6-μm homogeneous cell was prepared for UV tests. A HeNe laser was used to probe the electro-optic properties of the LC cell. From Fig.3, the extrapolated UV stability of PTP-5NCS is about 40 minutes at I~50mw/cm² exposure intensity, which is much better than that of the PTTP compounds. The absorption wavelengths of PTTP and PTP-5NCS are similar. Therefore, electronic transition wavelength is not the sole factor affecting the stability of the LC material. Molecular structure also plays an important role.

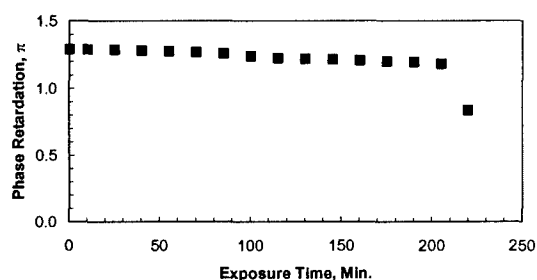


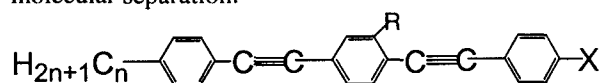
Fig.3 The measured phase retardation of a d~6-μm homogeneous cell containing 20% PTP-5NCS in ZLI-2359. UV intensity I~50mw/cm². λ=633nm.

LCs with $\Delta n > 0.5$

Two series of LC compounds with $\Delta n > 0.5$ at $\lambda = 589\text{nm}$ have been reported. They are bistolanes and isothiocyanato naphthalene tolans.

Bistolanes

Bistolanes¹² exhibit a high Δn due to their long molecular conjugation. However, as the conjugation length increases, their melting point also increases. Based on the Schröder-van Laar equation, high melting point leads to a poor solubility for forming eutectic mixtures. An effective way to lower melting point is to substitute a lateral alkyl group in the middle phenyl ring, as shown below, to widen the molecular separation:¹³



Here, X can be an F, CN or NCS group, and R can be a hydrogen, methyl, ethyl or fluoro group.

Table III lists the phase transition temperatures of some fluoro and cyano bistolanes. The compound with R=H has melting point as high as 173°C. Thus, its solubility is poor. With a fluoro substitution, the melting point is decreased to 146°C. In the case that R=CH₃, the melting point is reduced to 69°C. Continuing to increase the lateral side chain length, such as C₂H₅, will lower the melting point further, however, its viscosity increases substantially. The extrapolated Δn of a cyano bistolane (with R=CH₃) is 0.53.

As the molecular conjugation length increases, the LC becomes bulkier so that its viscosity also increases. To reduce viscosity, elevated temperature (40-50°C) operation has been commonly considered. Roughly speaking, the visco-elastic coefficient (γ_1/K) declines two times as the operating temperature increases by every 15°C.

Table III Phase transitions (in °C) and heat fusion enthalpy (kcal/mol) of some bistolanes.

n	R	X	T _{mp}	T _c	ΔH
4	H	F	173	207	7.6
4	F	F	146	170	6.5
5	Me	F	69	163	5.0
5	Et	F	61	103	5.2
5	Me	CN	114	203	5.5
5	Et	CN	85	159	3.5

The UV stability of a dialkyl bistolane PTP-TP-53 was studied. At I=50mw/cm² intensity, PTP-TP-53 can only withstand about 2 minutes of UV exposure. The photo stability of a LC is determined by its absorption wavelength and chemical structure. Fig.6 shows the absorption wavelength of three compounds studied: PTP-4F, PTP-5NCS and PTTP-52. During experiment, 1% of the guest compound was dissolved in an UV transparent LC mixture, ZLI-2359. A d~6μm homogeneous cell was used for the absorption measurements. From Fig.6, the absorption tail of PTTP-52 is on the edge of the central UV light. Thus, its UV stability is much worse than that of PTP-5NCS.

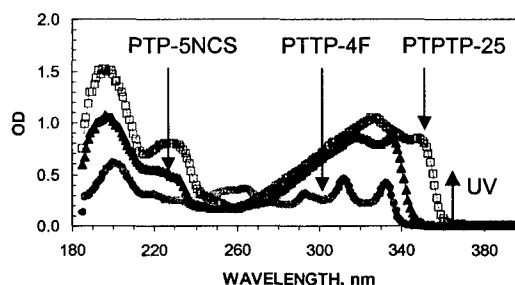
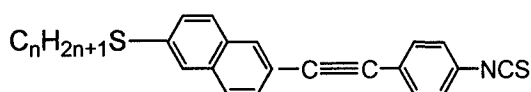


Fig.6 UV absorption spectra of PTTP-4F, PTP-5NCS and PTTP-52. Concentration=1%, cell gap d=6μm and host LC is ZLI-2359.

Also observed from Fig.6, the absorption tail of PTTP-4F and PTP-5NCS extends to 340nm and 350nm, respectively. Although PTP-5NCS has a slightly longer absorption, it can still withstand ~40 minutes of UV irradiation as compared to 30 seconds for PTTP-4F. Thus, chemical structure also plays an important role in determining the UV and thermal stability.

Isothiocyanato Naphthalene Tolanes

Another series of nematic LC with $\Delta n > 0.5$ is the isothiocyanato naphthalene tolane (with structure shown below) reported by the Hull University:¹⁴



The $n=4$ homologue shows $\Delta n \sim 0.54$ and nematic range from 91.5 to 136.7°C. The naphthalene group not only lengthens the molecular conjugation, but also suppresses the smectic phase. Its viscosity and photo and thermal stability have not been evaluated.

LC Absorption

Visible to Near IR

For high power laser beam steering in the near IR region, the LC absorption is a critical issue because some overtone molecular vibration bands exist. Two factors contribute to the optical loss: light scattering and absorption. To suppress light scattering, the LC mixture under study was heated to an isotropic state. In addition, in order to take surface reflections into consideration, a 1-mm gap quartz cell was used in the reference channel and a 2-cm cell used as sample. Therefore, the measured optical loss is equivalent to a 1.9-cm LC layer. For such absorption measurements, ~ 1 g of sample is required. Thus, we chose Merck E7 mixture ($T_c=60^\circ\text{C}$) for such studies. Both sample and reference cells were controlled at $T \sim 70^\circ\text{C}$. Results are depicted in Fig.7.

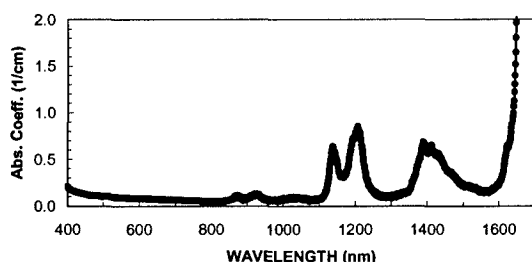


Fig.7 Measured absorption coefficient of an E7 LC cell in the visible and near IR regimes. $T \sim 70^\circ\text{C}$. $d=1.9\text{-cm}$.

From Fig.7, E7 has relatively small absorption in the visible region. This is because the $\pi \rightarrow \pi^*$ electronic transitions of E7 are located in the UV region. As the wavelength gets further apart from resonance, absorption decreases. The absorption minimum occurs at near IR ($\lambda \sim 850\text{nm}$) region. At $\lambda=1.06\mu\text{m}$, $\alpha \sim 0.08\text{ cm}^{-1}$. Thus, the LC-based OPA should be able to steer high power YAG laser beams. Usually, in a LC panel, the conductive and transparent ITO layer has the lowest damage threshold ($\sim 200\text{MW/cm}^2$). To avoid laser-induced phase transition to occur, a high T_c LC mixture is recommended.

Beyond $\lambda=1.1\mu\text{m}$, the overtone vibration bands appear. At $\lambda=1.3$ and $1.55\mu\text{m}$ (two laser wavelengths commonly used for fiber-optic communications), the LCs we studied all exhibit absorption valleys.¹⁵ At these two wavelengths, the absorption coefficients of E7 are 0.1 and $0.15/\text{cm}$, respectively. Suppose a $5\text{-}\mu\text{m}$ cell gap is used for the $\lambda=1.55\mu\text{m}$ optical switch, the absorption loss is quite negligible.

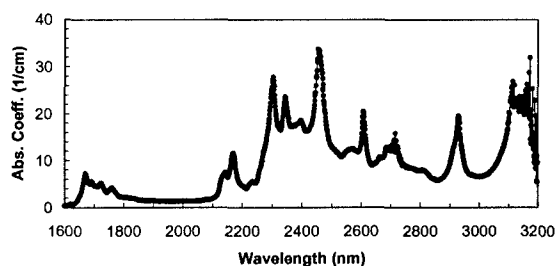


Fig.8 Measured IR absorption coefficient of an E7 LC cell at $T \sim 70^\circ\text{C}$. $d=1.9\text{cm}$.

Mid IR

In the longer IR region ($\lambda > 2.1\mu\text{m}$), several overtone molecular vibration bands exist and overlap closely. As a result, the background absorption coefficient reaches $\alpha \sim 10\text{cm}^{-1}$, as shown in Fig.8. For a $5\text{-}\mu\text{m}$ cell, the absorption loss accounts for 0.5%. The absorbed laser light will be converted to heat and warm up the LC medium.

Conclusions

We have developed several high birefringence ($\Delta n > 0.4$) LC compounds for laser beam steering application. It is generally true that in order to enhance birefringence, the molecular conjugation length needs to be increased. Three side effects on increasing conjugation length have been found: high melting temperature, increased viscosity, and decreased UV stability. Therefore, an optimal molecular structure should exist for balancing all the required physical properties, such as nematic range, birefringence, viscosity, operating voltage, optical loss, and material stability. Molecular modeling and simulations before compound synthesis are highly desirable.

Acknowledgment

This work was partially supported by AFOSR under contract number F49620-98-C-0019. The author is indebted to Dr. Terry Dorschner of Raytheon for technical discussions and W. H. Smith, Jr. of HRL Lab. for skillful technical assistance.

References

1. P. F. McManamon et al, Proc. IEEE 84, 268 (1996)
2. S. T. Wu and D. K. Yang, "Reflective Liquid Crystal Displays" (Wiley, Chichester, 2001).
3. S. T. Wu, Phys. Rev. 33, 1270 (1986).
4. I. Haller, Prog. Solid State Chem., 10, 103 (1976).
5. S. T. Wu et al, Appl. Phys. Lett. 61, 635 (1992).
6. S. T. Wu et al, Appl. Phys. Lett. 77, 957 (2000).
7. M. D. Wand et al, Ferroelectrics 180, 333 (1996).
8. S. T. Wu, US patent pending.
9. G. W. Gray et al, MCLC 37, 213 (1976).
10. C. Sekine et al, MCLC 332, 235 (1999).
11. Y. B. Kim and B. H. Kim, SID Tech. Digest, 31, 874 (2000).
12. Y. Goto and K. Kitano, EP 345,013 (1989).
13. S. T. Wu et al, JJAP 39, L38 (2000).
14. A. J. Seed et al, J. Mater. Chem., 10, 2069 (2000).
15. S. T. Wu, J. Appl. Phys. 84, 4462 (1998).